

Large scale structures in liquid crystal/clay colloids

This article has been downloaded from IOPscience. Please scroll down to see the full text article.

2005 J. Phys.: Condens. Matter 17 2255

(<http://iopscience.iop.org/0953-8984/17/15/001>)

View [the table of contents for this issue](#), or go to the [journal homepage](#) for more

Download details:

IP Address: 129.252.86.83

The article was downloaded on 27/05/2010 at 20:37

Please note that [terms and conditions apply](#).

Large scale structures in liquid crystal/clay colloids

Jeroen S van Duijneveldt¹, Susanne Klein², Edward Leach²,
Claire Pizzey¹ and Robert M Richardson³

¹ School of Chemistry, Cantock's Close, University of Bristol, Bristol BS8 1TS, UK

² HP Laboratories, Filton Road, Stoke Gifford, Bristol BS34 8QZ, UK

³ H H Wills Physics Laboratory, Tyndall Avenue, University of Bristol, Bristol BS8 1TL, UK

Received 24 November 2004, in final form 10 March 2005

Published 1 April 2005

Online at stacks.iop.org/JPhysCM/17/2255

Abstract

Suspensions of three different clays in K15, a thermotropic liquid crystal, have been studied by optical microscopy and small angle x-ray scattering. The three clays were claytone AF, a surface treated natural montmorillonite, laponite RD, a synthetic hectorite, and mined sepiolite. The claytone and laponite were sterically stabilized whereas sepiolite formed a relatively stable suspension in K15 without any surface treatment. Micrographs of the different suspensions revealed that all three suspensions contained large scale structures. The nature of these aggregates was investigated using small angle x-ray scattering. For the clays with sheet-like particles, claytone and laponite, the flocs contain a mixture of stacked and single platelets. The basal spacing in the stacks was independent of particle concentration in the suspension and the phase of the solvent. The number of platelets in the stack and their percentage in the suspension varied with concentration and the aspect ratio of the platelets. The lath shaped sepiolite did not show any tendency to organize into ordered structures. Here the aggregates are networks of randomly oriented single rods.

1. Introduction

Organically modified 2:1 layering clays have a tendency to organize into stacks of a number of platelets when dispersed into organic solvents (e.g. Theng 1979, Ho *et al* 2001). When dispersing such platelets into a thermotropic liquid crystal we observed the same behaviour (Pizzey *et al* 2004), particularly for platelets with a high aspect ratio, for example sterically stabilized montmorillonite particles with a diameter between 0.5 and 1 μm . Small angle x-ray scattering (SAXS) revealed that these platelets dispersed in K15 (4-pentyl-4'-cyanobiphenyl) form stacks of 5 ± 2 platelets with a basal layer spacing of 37 Å independent of the temperature and concentration of the suspension. The spacing and stack size is however influenced by the host. The non-mesogenic host toluene favoured a higher percentage of single platelets and the stacks formed had on average two platelets with a basal layer spacing of 48 Å.

Particles with a smaller aspect ratio, for example sterically stabilized laponite, a synthetic hectorite of 1 nm thickness and ~ 26 nm diameter, appeared to delaminate almost completely in both solvents. Only 10% of the particles were found in stacks of 2 ± 1 platelets with the same spacings as for montmorillonite, i.e. 37 \AA in K15 and $52 \pm 7 \text{ \AA}$ in toluene.

The minimum scattering vector, Q , probed in these experiments was 0.03 \AA^{-1} so it was not possible to determine whether the stacks and platelets were isolated or part of a larger aggregates. In this paper we report SAXS measurements extended to a lower Q range ($0.003\text{--}0.3 \text{ \AA}^{-1}$) to investigate the possibility of larger scale aggregation. The low Q was achieved using station 2.1 at the Daresbury Synchrotron Radiation Source (Daresbury) and beamline BM02 at the ESRF in Grenoble (Grenoble) rather than the laboratory based SAXS apparatus employed in the previous work. Furthermore, the high intensity of synchrotron radiation allowed short measurement times so that the flocculation could be monitored as a function of time. In addition, results are presented on suspensions of sepiolite, a naturally occurring clay consisting of lath shaped particles.

2. Sample preparation

Three types of clay were used. The two clays with plate-like particles have a similar chemical structure but differ greatly in aspect ratio.

Claytone AF is a surface treated natural montmorillonite clay with a thickness of approximately 1 nm and a range of diameters from 70 to 150 nm (Rockwood Additives). However, in SEM studies we found that the majority of particles had a diameter in the region of $1 \mu\text{m}$. The surface is treated with dihydrogenated tallow, a mixed surfactant, the major component of which is dimethyldioctadecylammonium bromide (DODAB) (Ho *et al* 2001), to give stable suspensions in non-aqueous solvents. The treated clay was cleaned repeatedly with a 40/60 mixture of propanol and water (ultra-pure, Millipore) to remove excess surfactant, dried under vacuum and finely ground prior to use.

Laponite RD (Rockwood Additives) is a synthetic hectorite type clay with a thickness of approximately 1 nm and a diameter of 25 nm (Rockwood Additives 2003). Laponite was totally dispersed in water (1 g, 1% w/w) by stirring for 24 h prior to surfactant treatment. The surfactant DODAB (Acros Chemicals, used as received) was added in dilute solution in an 80:20 water:propanol mix to give 100% coverage using a cationic exchange capacity (CEC) of 73 meq/100 g clay (Cione *et al* 1998). The treated clay was cleaned by repeated washing and was subsequently dried under vacuum to remove all traces of water (Jordan 1949). The particles were finely ground with an agate pestle and mortar and dried prior to suspension in the isotropic phase of the liquid crystal.

The third clay, the lath shaped clay sepiolite 60/120 (an industrial grade, Steetley Bentonite and Absorbants), consists of 80% sepiolite and 20% associated minerals. Organic contaminants were removed by washing the clay in 30% w/v hydrogen peroxide solution. 100 ml of hydrogen peroxide solution was added to 10 g of clay and stirred overnight after which gentle heating was applied to decompose all remaining hydrogen peroxide. The wet clay was then sieved through a sieve tower with decreasing retention from 500 to $38 \mu\text{m}$. One litre of de-ionized water was added and the clay–water suspension was filtered through a Whatman 5 paper filter with $2.5 \mu\text{m}$ retention. The clay was left to sediment, the supernatant liquid was removed and the remaining particles were dried under atmospheric conditions. The yield was 25%. The cleaning procedure leads to relatively mono-disperse sepiolite laths with an average length of 200 nm (see figure 1). Sepiolite was not treated with any steric stabilizer as it was found to suspend in liquid crystal in its native state. The 20% of associated minerals are mostly quartz which has a different aspect ratio and a different surface chemistry compared to sepiolite. Quartz particles

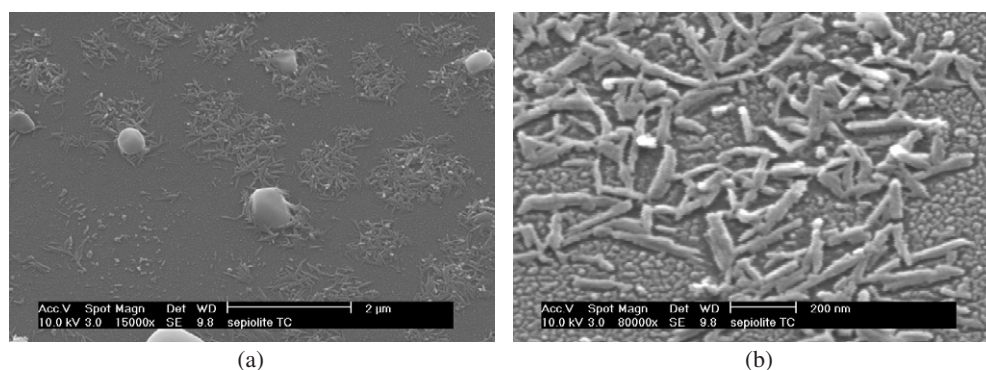


Figure 1. Sepiolite rods after cleaning and filtering. The quartz particles visible in the SEM micrographs on the left side could be separated chemically from the sepiolite particles. On the right, at higher magnification, the relatively mono-dispersed single laths can be seen.

smaller than $2.5 \mu\text{m}$ cannot be removed from the sepiolite laths by filtering (figure 1), but they will not contribute to the SAXS data since they cannot be dispersed in the organic solvents used in this study. The liquid crystal chosen was K15 (4-pentyl-4'-cyanobiphenyl, Merck, used as received) due to its high purity and room temperature nematic phase. The clays were suspended in K15 following three different suspension methods. The first step is the same for all three methods. Dried and finely ground clay is added to the isotropic liquid crystal.

Method 1 (M1)

The mixture is stirred for 60 min above the transition temperature and sonicated for 15 min in a 0.8 l Fisherbrand FB11020 with an operating power of 100 W emitted through two transducers located in the base. The sample is stirred for an additional 15 min and sonicated for a further 15 min.

Method 2 (M2)

The mixture is stirred for 15 min above the transition temperature and sonicated for 6–7 h.

Method 3 (M3)

To disperse the particles in a solvent we use a high shear mixer (IKA: Ultra Turrax T25) and drive it at 24 000 rpm for 3 min.

All preparation methods require degassing above the transition temperature in a vacuum oven at 60°C , 200 mbar for at least 4 h. The clearing temperature for all the samples was found to be the same as for pure K15, indicating that chemical contamination was negligible.

The suspensions are stable for up to 24 h in the nematic and the isotropic temperature regimes. After this time, flocculation and sedimentation are observed. The sample then developed two discrete layers, one particle poor and the other particle rich with an open floc structure. The aggregates were easily broken up; 15 min of stirring at approximately 40°C restored a good suspension.

3. Small angle x-ray scattering

The SAXS measurements were performed at the Synchrotron Radiation Source (SRS) at station 2.1 at the Daresbury Laboratory operating at a fixed wavelength ($\lambda = 1.5 \text{ \AA}$). The multiwire area detector was placed at 6.5 m from the sample to cover a Q range from 0.003 to

0.083 Å⁻¹ and at 1.25 m for a Q range of 0.027–0.43 Å⁻¹. The sample to detector distance was calibrated using rat tail collagen for the low Q range and a silver behenate standard (Huang *et al* 1993) for the higher Q range. Lindemann glass capillaries (diameter 2 mm, wall thickness 0.01 mm) which had been flattened to give a path length of ~1 mm for the x-ray beam were filled with the suspensions. The sample temperature was controlled in the range 25–65 °C by an electrical heater and the samples were cooled from the isotropic phase in a ~0.5 T magnetic field in order to induce alignment. The scattering was generally measured within a few minutes of sample preparation before detectable sedimentation had occurred.

The measured counts were corrected for the efficiency of each pixel by dividing the data by the counts from a ⁵⁵Fe radioactive source, which gave an isotropic flood of x-rays. The detector counts were then divided by the main beam intensity on the detector (i.e. the central peak intensity) after it had passed through the semi-transparent beam stop. This corrected for the variation of the incident intensity and the transmission of the samples.

Thus, the scattering from the liquid or liquid crystal host was subtracted from the scattering from the dispersions using the formula

$$I_{\text{correct}} = \frac{I_{L+P}}{C P_{L+P}} - \frac{I_L}{C P_L} \quad (1)$$

where I_{L+P} is the intensity from the dispersion (liquid + particles) in a sample tube and $C P_{L+P}$ is the central peak intensity of the dispersion in a sample tube. I_L and $C P_L$ are the corresponding quantities for a sample of the pure dispersion medium (solvent only). Since the dispersion only contains a few per cent of clay and the sample tubes were nominally the same thickness, this formula gives a reasonable correction for the scattering from the liquid host and the container. After the background correction, the data were azimuthally averaged in order to improve statistics and make the scattering from the isotropic and nematic phases comparable. The data sets for the two different detector settings were stitched together by scaling the high Q data set to coincide with the low Q data set in the overlap region.

Some of the data were taken at the European Synchrotron Radiation Facility using the BM02 station. The detector was a charge-coupled device so a no-beam background was first subtracted from the raw data. After that, the data processing was similar to that for station 2.1 except that the incident intensity and sample transmission were measured by the scattering from a thin polymer film placed after the sample at 45° to the beam.

4. Results

4.1. Claytone AF

The small angle scattering data from claytone suspended in K15 is shown in figure 2. The first and second order pseudo-Bragg peaks indicate the formation of stacks of platelets. The positions of these peaks were found to be independent of the clay concentration in the suspension, the temperature and preparation method. The scattering data in the Q -range between 0.03 and 0.4 Å⁻¹ were consistent with the model for a mixture of free platelets and stacks of platelets in the ‘large plate’ approximation. The formula (Pizzey *et al* 2004) for the scattering intensity, $I(Q)$, for this model is

$$I(Q) \approx \frac{S}{Q^2} \left(\frac{\sin Qh/2}{Qh/2} \right)^2 \left(((1-x)\langle \sin^2 M Qd/2 \rangle_M + x \sin^2 Qd/2) \left(\frac{1}{\sin Qd/2} - \frac{2\varphi}{Qd} \right)^2 \right) \quad (2)$$

where S is a scaling factor, h the thickness of the platelets, M the number of platelets in a stack, d the basal layer spacing within a stack and x the fraction of particles that are single

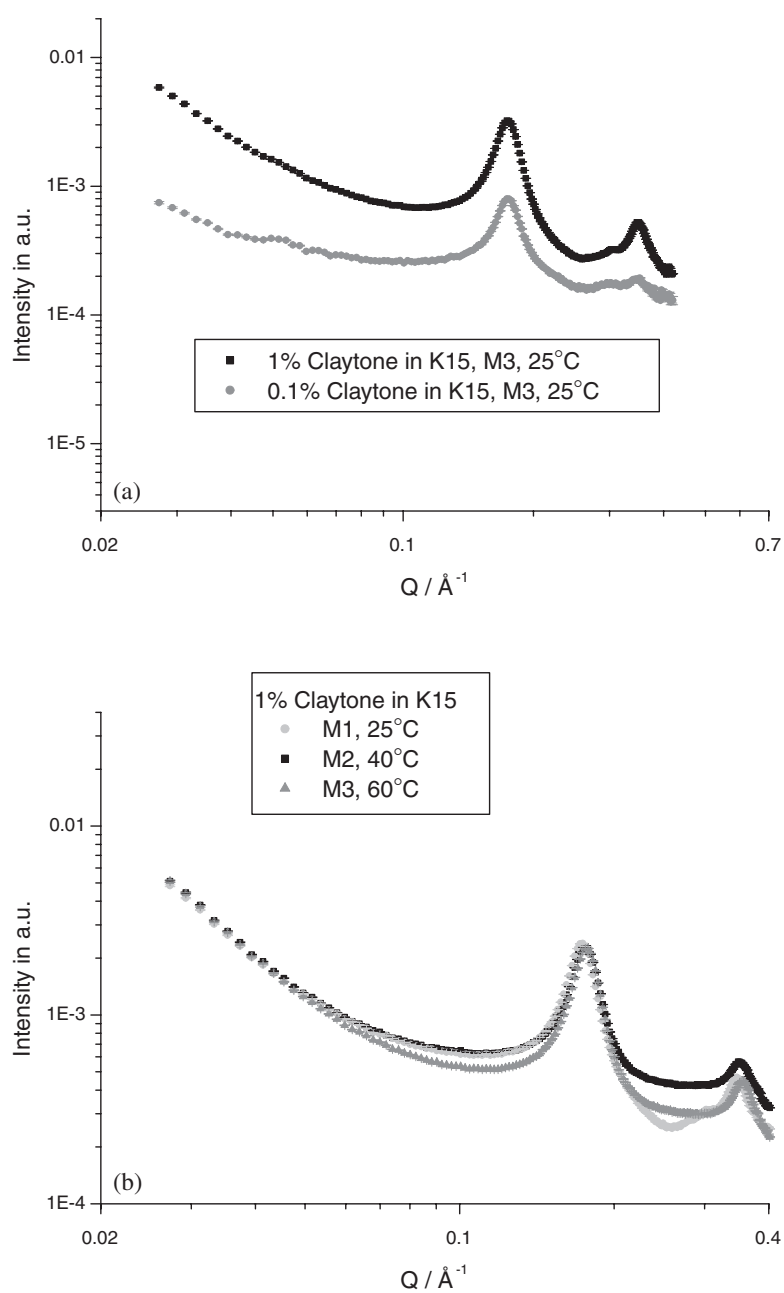


Figure 2. SAXS data of claytone in K15 over the higher Q range: (a) SAXS from 0.1% and 1% claytone in K15 shows that the position of the pseudo-Bragg peaks is independent of the concentration of particles in suspension. The small peak between the first and second order Bragg peaks could be caused by periodic spacing in some larger aggregate or by a problem with the background correction, i.e. the peak is the under-corrected K15 peak. It does not appear in all measurements and is therefore not related to the equilibrium spacing between the platelets in a stack. (b) SAXS from different 1% suspensions of claytone in K15 shows that preparation method and temperature do not influence the features in the scattering curve.

platelets rather than stacks, and ϕ adjusts the mean electron density of the surrounding of any particular stack of platelets.

Figure 3(a) shows a fit with a basal layer spacing of 35.4 Å, 4 ± 2 platelets in a stack and $21 \pm 2\%$ single platelets in the suspension the results are similar to those previously published (Pizzey *et al* 2004). Again the main features in the data are not changed by temperature or concentration and do not change with the preparation method. In this paper we focus on the lower Q scattering ($Q < 0.03 \text{ \AA}^{-1}$) which is sensitive to structures on a larger scale than single platelets or stacks.

For $Q < 0.03 \text{ \AA}^{-1}$ the gradient of the double-log plots of the scattering curves changes from -2 to -3 (figure 3(b)). A gradient of -2 is indicative of randomly oriented platelets with a high aspect ratio, whereas a gradient of -3 is indicative of scattering from fractal surfaces of large objects (Beaucage 1995, 1996) or from the interior of large objects with an entangled or network type of structure. In this case, the most likely large object is an aggregate of single discs or stacks. The large objects are definitely not large stacks (e.g. many more than four platelets) or other large agglomerates with close to 100% volume fraction. These would both give a gradient of -4 on these plots. The large object interpretation is supported by micrographs taken of a freshly made suspension between two glass platelets shown in figure 4 and by the shift of the cross-over point in figure 3(b). In a less concentrated suspension there will be a lesser tendency to aggregate. The result is a shift of the cross-over point to lower Q as discussed in a later section.

The aggregates seen in figure 4 are not the particles themselves because these are too small, but a combination of particles and liquid crystal domains around them that have a director orientation different to the bulk.

The clay particles are almost refractive index matched to the isotropic phase of K15 and are therefore invisible when the suspension is heated above the transition temperature. On cooling into the nematic, the matching condition is lost and the aggregates become visible. From the scale we deduce that they are at least $1 \mu\text{m}$ in size.

The original model of small stacks and free platelets (equation (2)) is in good agreement with the SAXS data in the region of $Q > 0.03 \text{ \AA}^{-1}$. At lower Q , the model predicts a zero order Bragg peak whose relative intensity is governed by the contrast parameter, ϕ , in equation (2). However, this peak appears as a gentle step in the Q^{-2} trend and does not reproduce a slope of Q^{-3} (see figure 3(a)). We have explored further modifications to this model such as a lateral displacement of the platelets in a stack but none were found that gave a Q^{-3} trend in the lower Q region. We are therefore confident that our assumption of a hierarchical model, with the small stacks and free platelets aggregated into larger scale objects, is fundamentally correct. The detailed arrangements of the stacks and platelets within these aggregates will be the subject of a future experimental investigation where we will follow concentration dependence in detail.

4.2. Laponite

The scattering data for the laponite suspensions showed a surprising feature. With a literature value for the plate diameter of 26 nm we expected to see a change of gradient in the log-log plots from -2 towards zero near $Q = 0.024 \text{ \AA}^{-1}$, but instead we found a deviation towards -3 near $Q = 0.01 \text{ \AA}^{-1}$ (figure 5). SAXS data from two different concentrations in the Q -range $Q > 0.03 \text{ \AA}^{-1}$ are in reasonable agreement with the model defined by values in table 1.

To fit the data at $Q > 0.03 \text{ \AA}^{-1}$ we used the model combining free and stacked platelets, but, unlike equation (2) above, the finite radius of the platelets is included. Hence the model

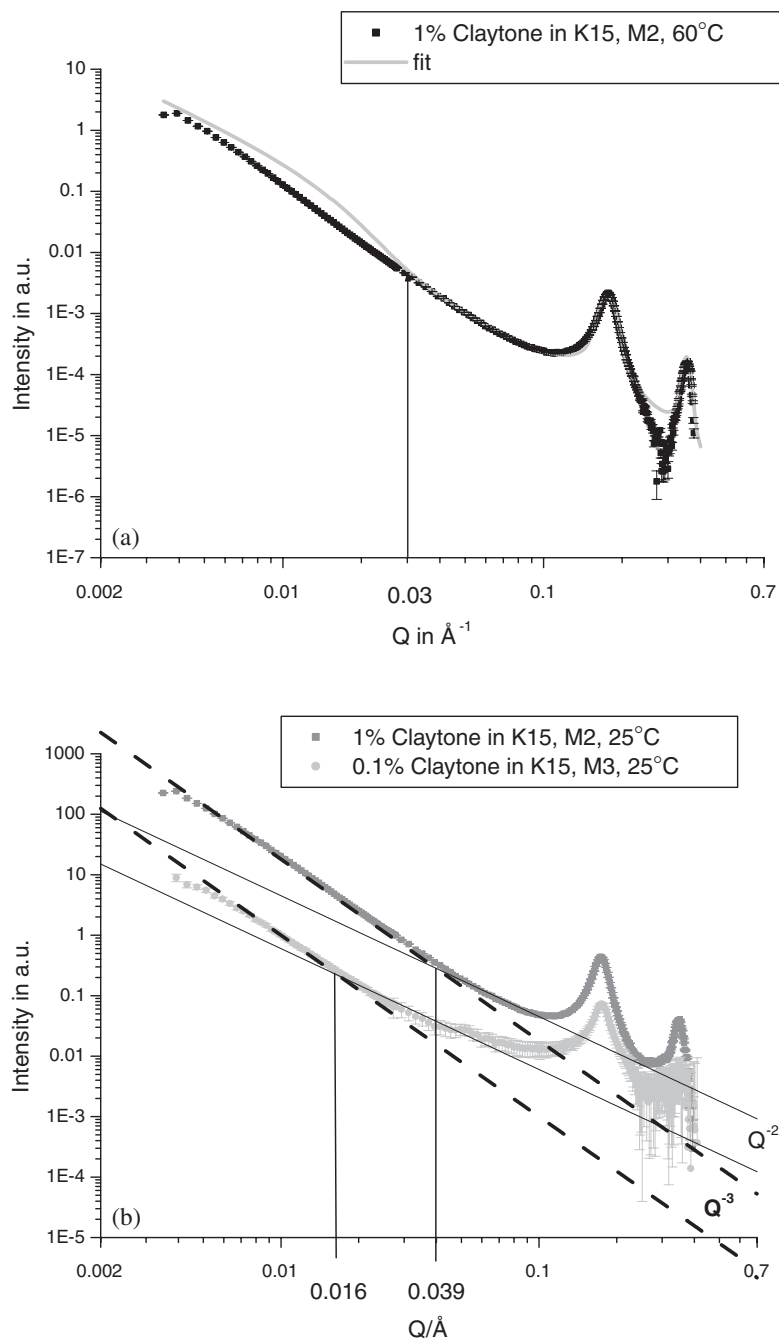


Figure 3. SAXS data of claytone over K15 in the combined Q range and fit. (a) The fit was obtained with the values $d = 35.4 \text{ \AA}$, $M = 4 \pm 2$, $21 \pm 2\%$ of single platelets in suspension. The plate thickness was fixed at 10 \AA . The model fits the data well in the region $Q > 0.03 \text{ \AA}^{-1}$, but deviates from the data for $Q < 0.03 \text{ \AA}^{-1}$. (b) The gradient of the log plots of the scattering data changes from -2 to -3 . The cross-over q values are indicated and shift with concentration.

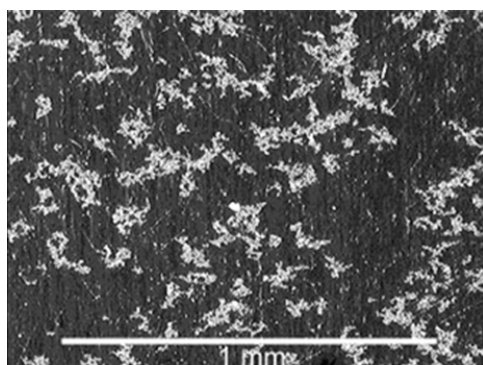


Figure 4. Micrograph of 1% claytone in K15 between two glass substrates. The sample thickness is approximately $100\ \mu\text{m}$. The substrate surfaces were treated with rubbed polyimide to align the liquid crystal parallel to the surfaces. The picture was taken between crossed polarizers.

scattering was calculated by numerical integration.

$$I(Q) = N_P \Delta\rho^2 \int_0^{\pi/2} F_a^2(Q \cos \theta) F_r^2(Q \cos \theta) \sin \theta \, d\theta \quad (3)$$

where for disc-like platelets the radial structure factor is given by an expression containing the first order Bessel function, J_1 ,

$$F_r(Q_R) = \pi r^2 \frac{2J_1(Q_R r)}{Q_R r} \quad (4)$$

where r is the radius of the disc. The axial structure factor is given by the expression

$$F_a^2(Q_Z) = \left(\frac{\sin Q_Z h/2}{Q_Z h/2} \right)^2 \left(((1-x) \langle \sin^2 M Q_Z d/2 \rangle_M + x \sin^2 Q_Z d/2) \times \left(\frac{1}{\sin Q_Z d/2} - \frac{2\varphi}{Q_Z d} \right)^2 \right) \quad (5)$$

where the symbols have the same meaning as for equation (2). Since the thickness is much less than the radius, this formula predicts the same change of gradient as the thin disc approximation (Kratky and Porod 1949) at the point where $Q \sim \pi/r$.

$$I(Q) \approx \frac{S}{Q^2 r^2} \left(1 - \frac{1}{Qr} J_1(2Qr) \right). \quad (6)$$

The parameters in the table below were selected to give a good agreement between equation (3) and the data for $Q > 0.03\ \text{\AA}^{-1}$. The scattering data below $0.03\ \text{\AA}^{-1}$ deviates from the curve for free and stacked discs (figure 5). In this range the data have a slope of about -3 rather than zero which indicates that there is some aggregate formation. As for claytone, the slope of -3 suggests a surface fractal of objects whose overall dimensions are too large to be determined by the data in the present Q range. The assembly of the platelets into large sheets cannot be excluded since laponite has a strong tendency to connect at the edges and the sheets would form large objects with fractal surfaces.

4.3. Sepiolite

The sepiolite particles are not sterically stabilized with added surfactant. Nevertheless, the suspensions are as stable as the surfactant treated laponite and claytone suspensions, i.e. it

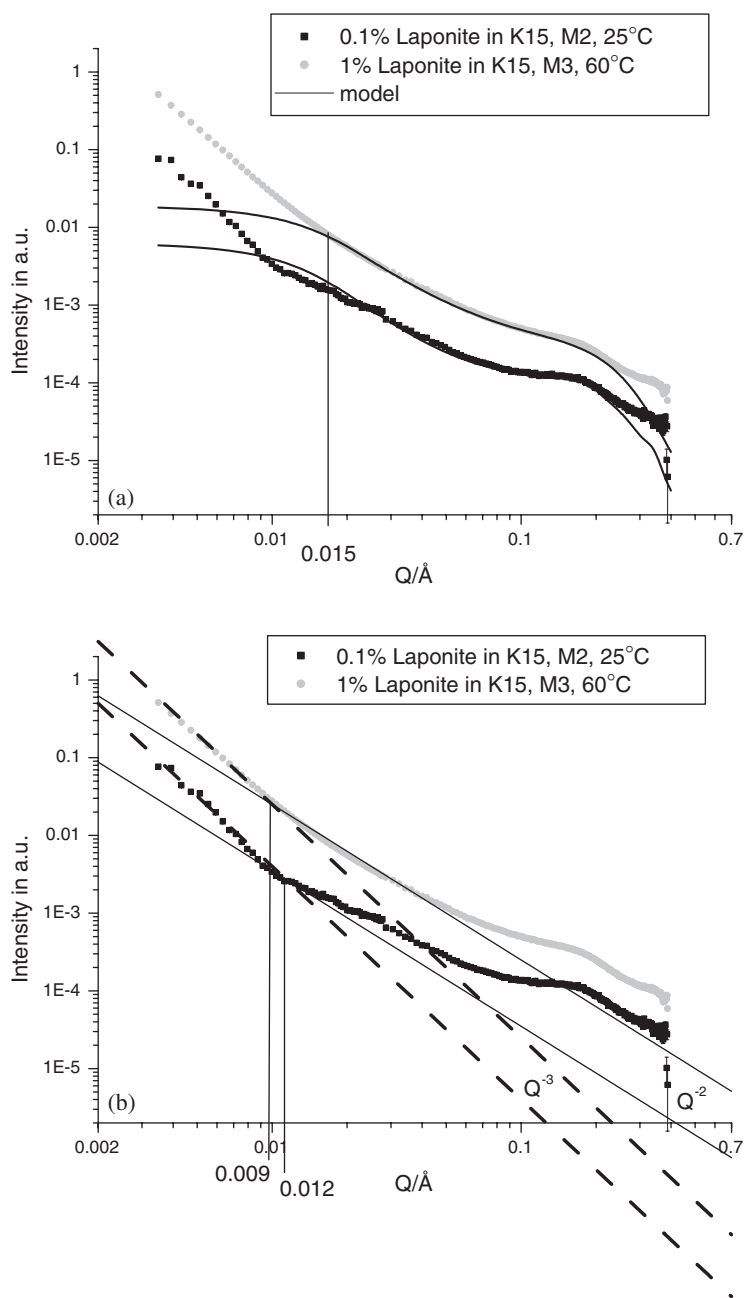


Figure 5. SAXS data of laponite in K15 over the combined Q range: (a) our model suggest for the data in the region $Q > 0.03 \text{\AA}^{-1}$ that laponite is mostly delaminated into single platelets of radius $\sim 150 \text{\AA}$ which is reflected in a change of gradient at $Q = 0.015 \text{\AA}^{-1}$; (b) the cross-over Q values between Q^{-3} and Q^{-2} behaviour are marked.

takes several hours before sedimentation becomes visible. We believe this is because of the high density of OH groups on its surface (Brauner and Preisinger 1956) which interact strongly with the liquid crystal molecules to form a stabilizing layer. Micrographs taken of a sepiolite suspension between two glass substrates show that the particles aggregate into flocs (figure 6).

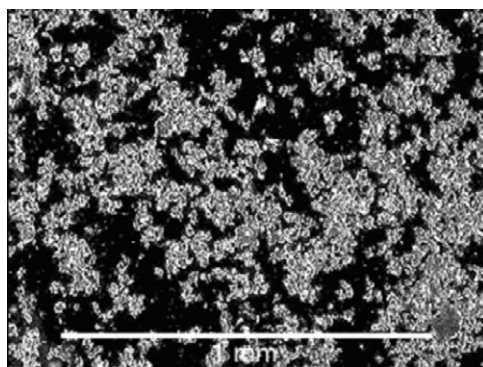


Figure 6. Freshly made suspension of 1% sepiolite in K15 between two glass substrates. The sample spacing is approximately 100 μm . On the two surfaces are layers of lecithin giving homeotropic alignment of the liquid crystal. The picture was taken between crossed polarizers.

Table 1. Parameters for clay suspensions in K15 optimized for the region $Q > 0.03 \text{ \AA}$.

	Radius of plate	Thickness of plate h	Basal layer spacing d	Number of platelets stack M	Percentage of single platelets	ϕ
1%						
Claytone	—	10 \AA^*	35.5 \AA	5 ± 2	21%	0.4
0.1%						
Claytone	—	10 \AA^*	35.5 \AA	2 ± 2	80%	0.8
0.1%						
Laponite	166 \AA^*	10 \AA^*	37 \AA	2 ± 1	92%	0.7
1%						
Laponite	145 \AA^*	10 \AA^*	37 \AA	2 ± 1	94%	0.6

* Assumed fixed values.

The scattering from 0.1% and 1% sepiolite in K15 shows a Q^{-3} trend at low Q and a cross-over to Q^{-1} at higher Q (figure 7). The Q^{-1} gradient is typical for rod shaped particles and Q^{-3} is expected from large aggregates with fractal surfaces.

4.4. Discussion of Q^{-3} scattering and cross-over points

We will now discuss the origin of the scattering that is proportional to a Q^{-3} power law in more detail. It should be noted that the scattering follows the power law from the beginning of the Q range observed in these experiments. This means that Q is not low enough to enter the Guinier region for the aggregate scattering and this implies that the aggregates are larger than $\sim\pi/Q_{\min}$, i.e. 1000 \AA . The scattering in the region $0.003 < Q (\text{\AA}^{-1}) < 0.03$ is therefore in an intermediate region where $1/Q$ corresponds to distances that are smaller than the whole aggregate. Since this Q range probes the interior of any object (i.e. an aggregate), the Q -dependence of the scattering is insensitive to the number of subunits (i.e. single or stacked platelets) that make up the whole object. It is therefore possible to relate the Q -dependence to the internal structure of the aggregate using the following scaling argument.

We may characterize any object by the relationship between its characteristic size or radius of gyration, R_g , and the number, z , of subunits of which it is composed. In general,

$$R_g \propto z^a \quad (7)$$

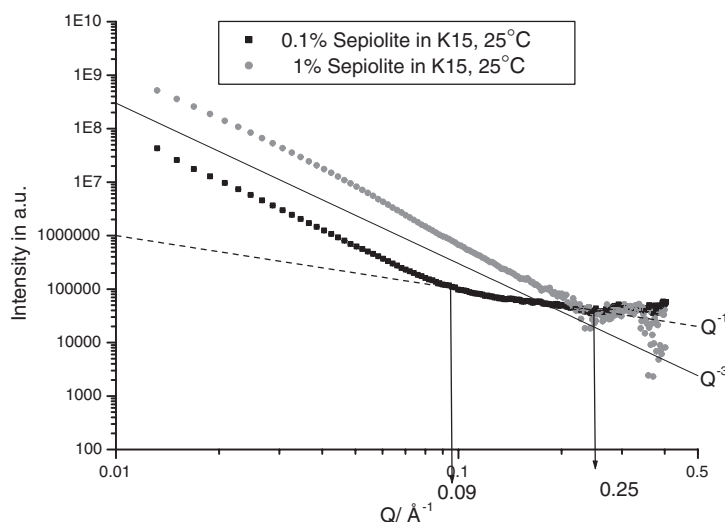


Figure 7. Scattering data for 0.1% and 1% sepiolite in K15. The scattering data in this figure were recorded at the ESRF in Grenoble, beamline BM02. The small peak at $Q = 0.32 \text{ \AA}^{-1}$ could not be reproduced in wide angle x-ray scattering measurements and is probably due to incomplete background correction. The cross-over Q values have been marked.

where for a rod shaped object it is well known that $a = 1$ and for a disc $a = 1/2$. For an open, three-dimensional network of linked rods or discs with a fixed volume fraction of subunits, $a = 1/3$. In the Q -range where the internal structure of an object is probed, the scattering is independent of z and a scaling argument (Higgins and Benoit 1994) may be used to show that the intensity, $I(Q)$, decays as a power law:

$$I(Q) \propto Q^{-1/a}. \quad (8)$$

Hence we have the well known results that for rods, $I(Q) \propto Q^{-1}$, for discs, $I(Q) \propto Q^{-2}$, and for the three-dimensional network, $I(Q) \propto Q^{-3}$.

Thus we propose that the internal structure of the large aggregates is an open network of platelets (for claytone and laponite) or rods (for sepiolite) with many contacts between these subunits.

If the suspensions consisted of aggregates of a fixed internal structure, the Q value for the cross-over from Q^{-3} to a weaker power law would be an indication of the distance between the contact points. For Q greater than the cross-over point, only one subunit is in the range being probed and so the scattering reverts to that of rods or (possibly stacked) platelets. However, in our data, we have found that the cross-over point varies with concentration. There are two possible explanations for this. Firstly, the internal structure of the aggregates could be changing with concentration. We might expect the contacts between the subunits to be further apart in dilute suspensions and this would shift the cross-over point to lower Q . Secondly, the suspensions may consist of free platelets and un-aggregated small stacks as well as the aggregates. The un-aggregated subunits would contribute scattering with the weaker power law and we might expect relatively more in dilute suspensions. This too would shift the cross-over to lower Q .

Since we have observed a shift of the cross-over to lower Q for the suspensions studied here, we can conclude that the platelets are rather weakly bonded into the aggregates and can respond to dilution either by changes of aggregate structure or by some re-dispersion of the aggregate.

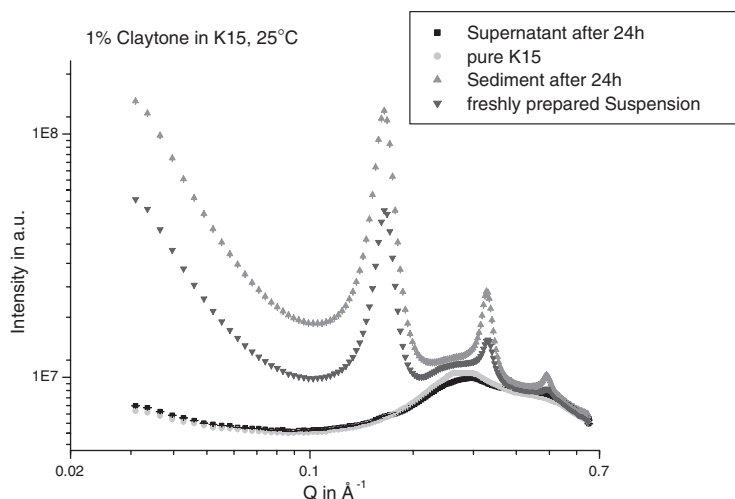


Figure 8. Time evolution of scattering data from 1% claytone in K15 at 25°C. After 24 h the scattering curves for the supernatant and pure K15 are identical, i.e. the supernatant is particle free. The scattering intensity in the particle rich phase increases by a factor of three, but the peak positions do not change.

For 1% solutions, we find $1/Q_{\text{cross}} \sim 30 \text{ \AA}$ for claytone and $\sim 67 \text{ \AA}$ for laponite. The distances calculated from the cross-over points are rather similar for claytone and laponite and are much less than the size of a claytone platelet. We have therefore a slight bias towards the second explanation. The observed shift to lower Q on dilution is most probably the result of some partial break up of the aggregates into single or stacked platelets.

4.5. Flocculation

A sample of 1% claytone in K15 was monitored over 24 h. SAXS measurements were made at different positions along the height of the capillary. After 24 h the scattering intensity from the translucent layer at the bottom of the capillary is three times more intense than the scattering intensity recorded from the ‘well dispersed’ suspension (figure 8). This is slightly more than expected from the volume ratio of the sediment over the whole sample. The peaks have neither shifted nor broadened. The self-organized structure of the platelets is therefore not affected by the sedimentation. The liquid crystal ‘drains’ from the structure. This explains why the suspension can be so easily re-dispersed when initially prepared successfully. The supernatant is virtually particle free. In figure 8 we have plotted scattering data for the freshly prepared suspension, the sediment and the supernatant without background correction next to scattering data from pure K15. It can be seen that the supernatant is identical to pure K15 and that the diffuse peak from the nematic is also visible in the freshly prepared suspension and the sediment at $Q \sim 0.26 \text{ \AA}^{-1}$. This suggests that the liquid remaining in the sediment is nematic K15. The absence of any isotropic material has been confirmed by NMR measurements (Luckhurst).

5. Conclusions

Claytone AF and laponite RD treated with DODAB only partially delaminate into single platelets when dispersed in the liquid crystal K15. Depending on the clay dimensions a varying proportion of the platelets self-organize into stacks. The basal layer spacing between

the platelets in a stack reaches equilibrium independent of concentration or temperature, i.e. state of solvent. All particles in suspension form large scale aggregates which finally lead to separation into a particle-free supernatant liquid and a particle rich sediment. During precipitation the basal layer spacing of the stacks remains unchanged and they can easily be re-dispersed. The supernatant and the liquid in the sediment show nematic ordering. This appears to be a different type of behaviour from that reported for spherical particles in nematic liquid crystals where the nematic order is disrupted and the isotropic phase is found below the normal transition temperature (Vollmer *et al* 2004). It seems that there is a higher compatibility between nematic ordering and platelets with homeotropic anchoring conditions.

The lath-like sepiolite does not show any stacking when suspended in K15. SAXS data reveals that single laths are randomly oriented in a network. Again this network is easily re-dispersed after flocculation and sedimentation.

The key to stable suspensions of plate or rod shaped particles in a nematic liquid crystal which do not disrupt the liquid crystalline order lies in understanding the equilibrium conditions for the stack formation and the prevention of large scale aggregates with randomly oriented particles.

Acknowledgments

The SAXS measurements were performed at the SRS in Daresbury and ESRF in Grenoble. We would like to thank Gunter Grossman (SRS) and Erik Geissler (ESRF) for their scientific support. The SEM micrographs were taken with the help of Steve Bodiley. One of the authors (CP) would like to thank EPSRC and the IMPACT-Faraday Ltd for financial support and Professor John Goodby for the kind donation of some of the 5CB used in this study.

References

- Beaucage G 1995 *J. Appl. Crystallogr.* **28** 717–28
Beaucage G 1996 *J. Appl. Crystallogr.* **29** 134–46
Brauner K and Preisinger A 1956 *Tschermaks Mineral. Petrog. Mitt.* **6** 120–40
Cione A P P *et al* 1998 *J. Colloid Interface Sci.* **198** 106–12
Daresbury 2004 http://srs.dl.ac.uk/info/STATION_INFO/stat2_1.html
Grenoble 2003 http://www.esrf.fr/exp_facilities/BM2/BM2.html
Higgins J S and Benoit H C 1994 *Polymers and Neutron Scattering* (Oxford: Oxford Science Publications)
Ho D L *et al* 2001 *Chem. Mater.* **13** 1923–31
Huang T C *et al* 1993 *J. Appl. Crystallogr.* **26** 180–4
Jordan J W 1949 *J. Phys. Colloid Chem.* **53** 294–06
Kratky O and Porod G 1949 *J. Colloid Interface Sci.* **4** 35–70
Luckhurst G R 2005 private communication, at press
Pizzey C *et al* 2004 *J. Phys.: Condens. Matter* **16** 2479–95
Rockwood Additives Product Information 2003
Theng B K G 1979 *Formation and Properties of Clay–Polymer Complexes* (New York: Elsevier)
Vollmer D *et al* 2004 *J. Phys.: Condens. Matter* **16** L227–33